Oxygen Atom Transfer, Coupled Electron−Proton Transfer, and Correlated Electron−Nucleophile Transfer Reactions of Oxomolybdenum(IV) and Dioxomolybdenum(VI) Complexes

Les J. Laughlin and Charles G. Young*

School of Chemistry, University of Melbourne, Parkville, Victoria 3052, Australia

Received June 29, 1995[⊗]

The oxo−Mo(IV) complexes $LMoO(S_2PR_2\text{-}S,S')$ [L = hydrotris(3,5-dimethylpyrazol-1-yl)borate; R = Me, Et, Pr^i, Ph] were prepared by reacting $MoO(S_2PR_2)_2$ and KL in refluxing toluene. The dioxo−Mo(VI) complexes *cis*-$LMoO_2(S_2PR_2\text{-}S)$ (R = Pr^i, Ph) were prepared by oxidation of the oxo−Mo(IV) complexes or by reaction of $LMoO_2Cl$ with NaS_2PR_2. Oxygen atom transfers from Me_2SO to $LMoO(S_2PR_2)$ were first-order with respect to Me_2SO and complex; the overall second-order rate constants at 40 °C range from $9.0(1) \times 10^{-5}$ $M^{-1}\cdot s^{-1}$ for $LMoO(S_2PMe_2)$ to $2.08(5) \times 10^{-4}$ $M^{-1}\cdot s^{-1}$ for $LMoO(S_2PPr_2)$; activation parameters were in the ranges $\Delta H^{\ddagger}$ = 63(1) to 73(1) kJ·mol^{-1}, $\Delta S^{\ddagger} = -88(1)$ to $-111(1)$ J·K^{-1}·mol^{-1}, and $\Delta G^{\ddagger} = 100(2)$ kJ·mol^{-1} for $LMoO(S_2PMe_2)$ to 98(2) kJ·mol^{-1} for $LMoO(S_2PPr_2)$. Oxygen atom transfer from pyridine *N*-oxide to $LMoO(S_2PPr_2)$ was also second-order with a rate constant of $1.54(5) \times 10^{-3}$ $M^{-1}\cdot s^{-1}$ at 40 °C, $\Delta H^{\ddagger} = 62(1)$ kJ·mol^{-1}, $\Delta S^{\ddagger} = -90(1)$ J·K^{-1}·mol^{-1}, and $\Delta G^{\ddagger} = 90(1)$ kJ·mol^{-1}. The second-order rate laws and large negative entropies of activation are consistent with associative mechanisms for the above reactions. Oxygen atom transfer from $LMoO_2(S_2PPr_2)$ to PPh_3 was first-order with respect to reactants, with an overall second-order rate constant of $2.5(3) \times 10^{-4}$ $M^{-1}\cdot s^{-1}$ at 30 °C. In toluene at 40 °C, all the above complexes catalyzed the oxidation of PPh_3 by Me_2SO, with turnover rates of ca. 0.9 mol of PPh_3/(mol of catalyst/h). Reduction of $LMoO_2(S_2PR_2)$ by SH^- led to the generation of the dioxo−Mo(V) anions $[LMoO_2(S_2PR_2\text{-}S)]^-$, which were slowly converted to the analogous oxothio−Mo(V) complexes $[LMoOS(S_2PR_2\text{-}S)]^-$. Dioxygen reacted with $[LMoOS(S_2PPr_2)]^-$ to produce the oxothio−Mo(VI) complex $LMoOS(S_2PPr_2\text{-}S)$. The (hydroxo)oxo−Mo(V) complexes $LMoO(OH)(S_2PR_2\text{-}S)$ were formed upon reduction of $LMoO_2(S_2PR_2)$ with PPh_3 in wet (3−5 M H_2O) tetrahydrofuran or upon ferrocenium oxidation of $LMoO(S_2PR_2)$ in wet tetrahydrofuran. In dry solvents, $LMoO(S_2PR_2)$ were oxidized to the corresponding cations, $[LMoO(S_2PR_2\text{-}S,S')]^+$, which reacted with water to form $LMoO(OH)(S_2PR_2)$. The Mo(V) complexes have been characterized by EPR spectroscopy.

Introduction

The pterin-containing molybdenum enzymes catalyze net oxygen atom transfer (OAT) reactions.[1−3] A possible mechanistic role for molybdenum-centered OAT was recognised in the early 1970s[4−6] and a wealth of molybdenum chemistry has developed around the oxo transfer hypothesis.[7,8] Indeed, single turnover experiments involving xanthine oxidase have confirmed that the oxygen atom transferred to xanthine arises from the molybdenum center exclusively.[9] As well, *Rhodobacter sphaeroides* dimethyl sulfoxide reductase catalyzes OAT from Me_2SO to 1,3,5-triaza-7-phosphatricyclo[3.3.1.1^{3,7}]decane;[10] this provides direct support for the oxo transfer hypothesis and justifies the development of enzyme models based on Mo-centered OAT reactions.

In the past decade, a number of catalytic OAT systems involving mononuclear dioxo−Mo(VI) and oxo−Mo(IV) complexes have been developed. The first, described by Holm and Berg,[8,11] employed the complexes $(L\text{-}NS_2)Mo^{VI}O_2$ and $(L\text{-}NS_2)Mo^{IV}O(DMF)$ [L-NS_2 = dianion of 2,6-bis(2,2-diphenyl-2-mercaptoethyl)pyridine, DMF = *N*,*N*-dimethylformamide]. OAT reactions involving a variety of phosphines and *S*- and *N*-oxides, including the biological substrates Me_2SO, *d*-biotin *S*-oxide, and nitrate, have been reported for these complexes.[11] The related complexes $(L\text{-}NS)_2Mo^{VI}O_2$ and $(L\text{-}NS)_2Mo^{IV}O$ [L-NS = bis(4-*tert*-butylphenyl)-2-pyridylmethanethiolate] also participate in clean OAT reactions.[12] Another system, reported by Roberts et al.,[13] was based on complexes of the type $LMo^{VI}O_2(S_2PR_2\text{-}S)$ and $LMo^{IV}O(S_2PR_2\text{-}S,S')$ [L = hydrotris(3,5-dimethylpyrazol-1-yl)borate (unless otherwise specified); R = alkoxy]. In this system OAT is accompanied by a change in the denticity of

[⊗] Abstract published in *Advance ACS Abstracts,* January 1, 1996.

(1) *Molybdenum Enzymes, Cofactors and Model Systems*, Stiefel, E. I., Coucouvanis, D., Newton, W. E., Eds.; ACS Symposium Series 535; American Chemical Society: Washington, DC, 1993.
(2) Enemark, J. H.; Young, C. G. *Adv. Inorg. Chem.* **1993**, *40*, 1.
(3) Young, C. G.; Wedd, A. G. *Encyclopedia of Inorganic Chemistry*; King, R. B., Ed.; Wiley: New York, 1994, p 2330 and references therein.
(4) Stiefel, E. I. *Proc. Nat. Acad. Sci. U.S.A.* **1973**, *70*, 988.
(5) Williams, R. J. P. *Biochem. Soc. Trans.* **1973**, *1*, 1.
(6) Garner, C. D.; Hyde, M. R.; Mabbs, F. E.; Routledge, V. I. *Nature* **1974**, *252*, 579.
(7) Holm, R. H. *Chem. Rev.* **1987**, *87*, 1401.
(8) Holm, R. H. *Coord. Chem. Rev.* **1990**, *100*, 183.
(9) Hille, R.; Sprecher, H. *J. Biol. Chem.* **1987**, *262*, 10914.
(10) Schultz, B. E.; Hille, R.; Holm, R. H. *J. Am. Chem. Soc.* **1995**, *117*, 827.
(11) (a) Holm, R. H.; Berg, J. M. *Pure. Appl. Chem.* **1984**, *56*, 1645. (b) Berg. J. M.; Holm, R. H. *J. Am. Chem. Soc.* **1985**, *107*, 917. (c) Berg, J. M.; Holm, R. H. *J. Am. Chem. Soc.* **1985**, *107*, 925. (d) Holm, R. H.; Berg, J. M. *Acc. Chem. Res.* **1986**, *19*, 363. (e) Harlan, E. W.; Berg. J. M.; Holm, R. H. *J. Am. Chem. Soc.* **1986**, *108*, 6992. (f) Caradonna, J. P.; Harlan, E. W.; Holm, R. H. *J. Am. Chem. Soc.* **1986**, *108*, 7856. (g) Caradonna, J. P.; Reddy, P. R.; Holm, R. H. *J. Am. Chem. Soc.* **1988**, *110*, 2139. (h) Craig, J. A.; Holm, R. H. *J. Am. Chem. Soc.* **1989**, *111*, 2111.
(12) (a) Gheller, S. F.; Schultz, B. E.; Scott, M. J.; Holm, R. H. *J. Am. Chem. Soc.* **1992**, *114*, 6934. (b) Schultz, B. E.; Gheller, S. F.; Muetterties, M. C.; Scott, M. J.; Holm, R. H. *J. Am. Chem. Soc.* **1993**, *115*, 2714.
(13) Roberts, S. A.; Young, C. G.; Cleland, W. E., Jr.; Ortega, R. B.; Enemark, J. H. *Inorg. Chem.* **1988**, *27*, 3044.

0020-1669/96/1335-1050$12.00/0

the dithiophosphate ligand. In all three systems, steric protection of the metal center is important in the prevention of comproportionation and dinucleation reactions leading to biologically unimportant Mo(V) species. More recently, Das et al.[14] and Nakamura and co-workers[15] described catalytic OAT reactions involving the complexes $[Mo^{IV}OL_2]^{2-}$ and $[Mo^{VI}O_2L_2]^{2-}$ [L = $S_2C_2(CN)_2^{2-}$, o-$S_2C_6H_4^{2-}$], and Arzoumanian et al.[16] reported that $[Mo^{IV}O(NCS)_4]^{2-}$ and $[Mo^{VI}O_2(NCS)_4]^{2-}$ catalyze OAT from Me_2SO to PPh_3. In these systems, the charge of the anions appears to play an important role in the prevention of comproportionation and dinucleation reactions. Finally, Purohit et al.[17] have reported that OAT reactions interconvert mononuclear Mo(IV) and Mo(VI) thiosemicarbazone complexes without producing dinuclear Mo(V) complexes.

Coupled electron−proton transfer (CEPT) reactions[2−4] appear to play a role in the reactivation of the molybdoenzymes after the OAT step and in the generation of the mononuclear, EPR-active Mo(V) states.[2,18] However, few valid models for these CEPT reactions are available[2,3] and in only one system has the marriage of both OAT and CEPT reactions, a feature of the biological systems, been achieved.[19] *cis*-Dioxo−, *cis*-(hydroxo)-oxo−, *cis*-oxothio−, and *cis*-(hydrosulfido)oxo−Mo(V) species have been targeted as models of the Mo(V) enzyme centers, or as synthetic precursors thereof. Dioxo−Mo(V) complexes have been synthesized by reduction of the corresponding Mo(VI) species,[19−22] oxothio−Mo(V) complexes by oxo-by-thio ligand exchange at dioxo−Mo(V) centers,[20,21] and (hydroxo)oxo− and (hydrosulfido)oxo−Mo(V) complexes by the protonation of the aforementioned $[Mo^{V}OE]^{+}$ (E = O, S) species.[19−21] The oxidation of Mo(IV) precursors is a virtually unexplored route to enzymatically relevant Mo(V) complexes. Indeed, one-electron oxidation of the $[MoO]^{2+}$, $[MoS]^{2+}$, and *trans*-$[MoO_2]$ complexes which dominate Mo(IV) chemistry does not permit direct access to such species; oxidation must be associated with elaboration of the coordination sphere by, for example, nucleophilic attack at the metal by water or hydroxide. This correlated electron−nucleophile transfer (CENT) strategy, summarized in eqs 1 and 2, is exploited here to generate enzymatically relevant (hydroxo)oxo−Mo(V) complexes.

$$[Mo^{IV}O]^{2+} \rightarrow [Mo^{V}O]^{3+} + e^{-} \quad (1)$$

$$[Mo^{V}O]^{3+} + H_2O \rightarrow [Mo^{V}O(OH)]^{2+} + H^{+} \quad (2)$$

In the system described by Xiao et al.,[19] oxidation of a putative (aqua)oxo−Mo(IV) species generates an (hydroxo)-oxo−Mo(V) species via CEPT; aquation followed by CEPT (eqs 3 and 4) effects the same net reaction as CENT. The mechanism adopted will be dictated by the other ligands at the metal center and their lability at the various oxidation levels.

$$[Mo^{IV}O]^{2+} + H_2O \rightarrow [Mo^{IV}O(H_2O)]^{2+} \quad (3)$$

$$[Mo^{IV}O(H_2O)]^{2+} \rightarrow [Mo^{V}O(OH)]^{2+} + H^{+} + e^{-} \quad (4)$$

These strategies may permit the generation of mononuclear oxo−Mo(V) complexes which are for various reasons inaccessible via the reduction of Mo(VI) precursors. As well, in view of the greater synthetic access to thio−Mo(IV) and −Mo(V) complexes,[2] CENT strategies may prove valuable in the systematic generation and isolation of $[Mo^{V}OS]^{+}$ and $[Mo^{V}O(SH)]^{2+}$ complexes.

Herein, we report the synthesis and characterization of dithiophosphinate complexes of the type $LMo^{IV}O(S_2PR_2\text{-}S,S')$ (R = Me, Et, Pr^i, Ph) and *cis*-$LMo^{VI}O_2(S_2PR_2\text{-}S)$ (R = Pr^i, Ph), kinetics studies of their OAT reactions, and their conversion to EPR-active $[Mo^{V}O]^{3+}$, $[Mo^{V}O_2]^{+}$, $[Mo^{V}O(OH)]^{2+}$, and $[Mo^{V}OS]^{+}$ complexes by CEPT and CENT reactions. As well, in chemistry pertinent to the reactivation of desulfo xanthine oxidase, we describe the first successful conversion of a dioxo−Mo(VI) complex to an oxothio−Mo(VI) complex via successive reduction, sulfurization and oxidation reactions. A wide variety of biologically important centers and processes are modeled by the chemistry described herein (Scheme 1).

Scheme 1

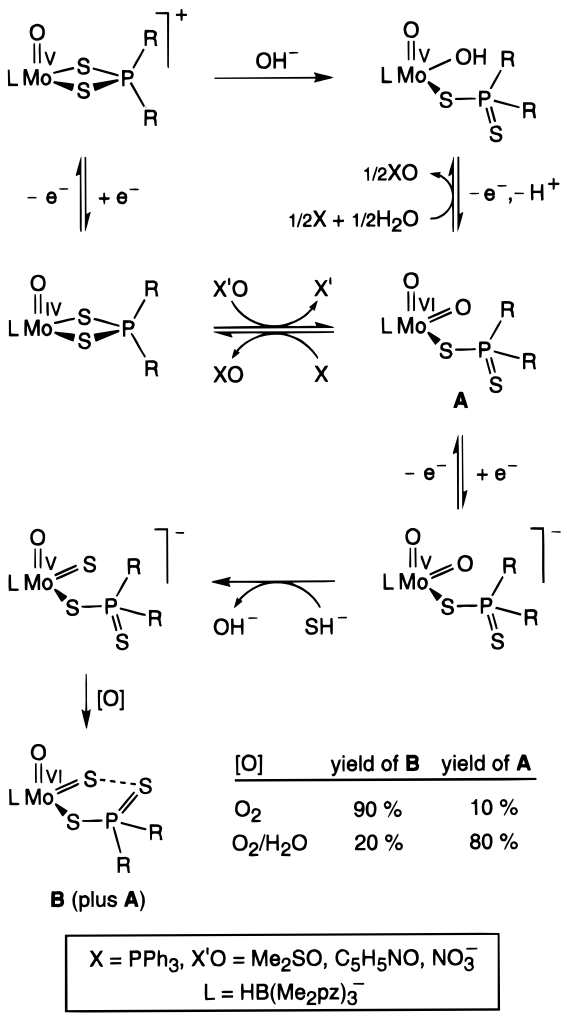

(14) Das, S. K.; Chaudhury, P. K.; Biswas, D.; Sarkar, S. *J. Am. Chem. Soc.* **1994**, *116*, 9061.
(15) (a) Yoshinaga, N.; Ueyama, N.; Okamura, T.; Nakamura, A. *Chem. Lett.* **1990**, 1655. (b) Nakamura, A. Private communication.
(16) Arzoumanian, H.; Lopez, R.; Agrifoglio, G. *Inorg. Chem.* **1994**, *33*, 3177.
(17) Purohit, S.; Koley, A. P.; Prasad, L. S.; Manoharan, P. T.; Ghosh, S. *Inorg. Chem.* **1989**, *28*, 3735.
(18) Bray, R. C. *Q. Rev. Biophys.* **1988**, *21*, 299.
(19) Xiao, Z.; Young, C. G.; Enemark, J. H.; Wedd, A. G. *J. Am. Chem. Soc.* **1992**, *114*, 9194.
(20) (a) Hinshaw, C. J.; Spence, J. T. *Inorg. Chim. Acta* **1986**, *125*, L17. (b) Dowerah, D.; Spence, J. T.; Singh, R.; Wedd, A. G.; Wilson, G. L.; Farchione, F.; Enemark, J. H.; Kristofzski, J.; Bruck, M. *J. Am. Chem. Soc.* **1987**, *109*, 5655. (c) Wilson, G. L.; Greenwood, R. J.; Pilbrow, J. R.; Spence, J. T.; Wedd, A. G. *J. Am. Chem. Soc.* **1991**, *113*, 6803. (d) Greenwood, R. J.; Wilson, G. L.; Pilbrow, J. R.; Wedd, A. G. *J. Am. Chem. Soc.* **1993**, *115*, 5385. (e) Wedd, A. G.; Spence, J. T. *Pure Appl. Chem.* **1990**, *62*, 1055.
(21) Xiao, Z.; Bruck, M. A.; Doyle, C.; Enemark, J. H.; Grittini, C.; Gable, R. W.; Wedd, A. G.; Young, C. G. *Inorg. Chem.* **1995**, *34*, 5950.
(22) (a) Xiao, Z.; Gable, R. W.; Wedd, A. G.; Young, C. G. *J. Chem. Soc., Chem. Commun.* **1994**, 1295. (b) Xiao, Z.; Gable, R. W.; Wedd, A. G.; Young, C. G. *J. Am. Chem. Soc.*, in press.

Experimental Section

Materials and Methods. Unless otherwise stated, all reactions were performed under an atmosphere of dinitrogen using standard Schlenk techniques and dried, distilled and deoxygenated solvents. Solvents employed in EPR experiments were rigorously dried and distilled over activated alumina just prior to use. Potassium hydrotris(3,5-dimethylpyrazol-1-yl)borate (KL),[23] HS_2PR_2 or NaS_2PR_2,[24] $MoO_2(S_2PR_2)_2$[25] and $[FeCp_2]PF_6$[26] ($Cp = \eta^5$-$C_5H_5^-$) were prepared by literature methods. Oxygen gas was dried by slow passage over 4 Å molecular sieves. All other reagents were AR grade or above. Infrared spectra were recorded on a Perkin Elmer 1430 spectrophotometer as pressed KBr disks. Proton and $^{31}P\{^1H\}$-NMR were obtained using Varian FT Unity-300 and Bruker FT AM300 instruments and were referenced to internal $CHCl_3$ (δ 7.26) and external 85% H_3PO_4 (δ 0), respectively. X-Band EPR spectra were recorded on Bruker FT ECS-106 and Varian E-line spectrometers using 1,1-diphenyl-2-picrylhydrazyl as reference. Electronic spectra were obtained on Shimadzu UV-240 and Hitachi 150-20 UV instruments using quartz cells. Electrochemical experiments were performed using a Cypress Electrochemical System II with a 3 mm glassy carbon working electrode and platinum auxiliary and reference electrodes. Solutions of the complexes (1−2 mM) in 0.1 M $NBu^n_4BF_4$/acetonitrile were employed and potentials were referenced to internal $LMoOCl_2$ at −0.351 V vs a saturated calomel electrode (SCE). Potentials are reported relative to the SCE. Chromatography was performed on a 50 cm column (2 cm diameter) using Merck Art. 7734 Kieselgel 60. Mass spectra were recorded on a Vacuum Generators VG ZAB 2HF mass spectrometer. Microanalyses were performed by Atlantic Microlabs, Norcross, GA.

Preparation of Compounds. $LMo^{IV}O(S_2PR_2$-*S,S′*). R = Me. A solution of NaS_2PMe_2 (3.25 g, 22 mmol) in water (40 mL) was added to a solution of $MoCl_5$ (2.0 g, 7.32 mmol) in 6 N HCl (13 mL) and the mixture was stirred for 30 min in air. The purple solid was isolated, washed with water and then ethanol, and vacuum dried. The dry solid was extracted into toluene (350 mL), the solution filtered, and the filtrate reduced to dryness to yield $Mo_2O_3(S_2PMe_2)_4$. This compound (1.3 g, 1.8 mmol) and PPh_3 (0.46 g, 1.8 mmol) were then refluxed in toluene (50 mL) for 1 h. The mixture was cooled, KL (1.3 g, 3.9 mmol) was then added, and the mixture was refluxed for a further 16 h. The mixture was filtered and the filtrate was reduced to dryness and chromatographed (silica/CH_2Cl_2) to give a green fraction. The solvent was removed in vacuo, and the residue was extracted using several portions of methanol (to remove $OPPh_3$). The complex was recrystallized with minimum delay from dichloromethane/methanol as green crystals. Yield: 0.67 g (35%).

Although spectroscopically pure, the compound yielded poor microanalytical results.

IR (KBr): 2960 m, 2920 s, 2525 m, 1540 s, 1440 s, 1410 s, 1380 s, 1370 s, 1290 m, 1280 m, 1210 s, 1060 s, 1040 m, ν(MoO) 960 vs, 900 m, 850 m, 810 m, 770 s, 720 s, 690 s, 640 s, 570 s, 500 m, 460 m, 350 m, 290 s cm^{-1}.

R = Et. A mixture of $MoO_2(S_2PEt_2)_2$ (0.7 g, 1.61 mmol) and PPh_3 (0.423 g, 1.61 mmol) in toluene (40 mL) was refluxed for 1 h. The mixture was then cooled, treated with KL (0.60 g, 1.77 mmol), and refluxed for a further 12 h. The reaction mixture was filtered and the filtrate was reduced to low volume. Chromatography on silica using dichloromethane as eluent yielded a main green fraction, which was recrystallized from dichloromethane/methanol. Yield: 0.71 g (78%).

Anal. Calcd for $C_{19}H_{32}BMoN_6OPS_2$: C, 40.58; H, 5.74; N, 14.94; S, 11.40. Found: C, 40.50; H, 5.78; N, 14.80; S, 11.35. IR (KBr): 2960 m, 2930 s, 2525 m, 1540 s, 1450 s, 1420 s, 1380 s, 1370 s, 1210 s, 1060 s, 1040 m, ν(MoO) 960 s, 860 m, 820 m, 790 s, 770 m, 700 m, 670 m, 650 m, 460 m, 350 m, 290 s cm^{-1}. Cyclic voltammetry (CH_3CN): $E_{1/2}$ +0.44 V, ΔE_{pp} 59 mV, I_{pa}/I_{pc} 1.05.

R = Pr^i. A mixture of $MoO_2(S_2PPr^i_2)_2$ (0.98 g, 2.1 mmol) and PPh_3 (0.525 g, 2.1 mmol) in toluene (50 mL) was refluxed for 1 h. Upon cooling, the mixture was treated with KL (0.74 g, 2.2 mmol) and then refluxed for a further 20 h. The jade green compound was isolated and purified by the methods described above for $LMoO(S_2PEt_2)$. Yield: 0.91 g (75%).

Anal. Calcd for $C_{21}H_{36}BMoN_6OPS_2$: C, 42.72; H, 6.15; N, 14.23; S, 10.86. Found: C, 42.77; H, 6.16; N, 14.19; S, 10.78. IR (KBr): 2960 s, 2920 s, ν(BH) 2520 m, 1545 s, 1445 s, 1410 s, 1375 s, 1365 s, 1200 s, 1060 s, 1035 s, ν(MoO) 950 s, 875 m, 855 m, 812 s, 790 s, 775 m, 690 m, 640 s, 615 s, 460 w, 290 s cm^{-1}. Mass spectrum: *m/z* 592 (100%). Cyclic voltammetry (CH_3CN): $E_{1/2}$ +0.40 V, ΔE_{pp} 69 mV, I_{pa}/I_{pc} 1.08.

R = Ph. A solution of $MoO_2(S_2PPh_2)_2$ (3.9 g, 6.22 mmol) and PPh_3 (1.8 g, 6.85 mmol) in toluene (80 mL) was refluxed for 1 h, cooled to room temperature, treated with KL (2.31 g, 6.85 mmol), and then refluxed for a further 5 h. The light green compound was isolated and purified by the methods described above for $LMoO(S_2PEt_2)$. Yield: 3.4 g (83%).

Anal. Calcd for $C_{27}H_{32}BMoN_6OPS_2$: C, 49.25; H, 4.90; N, 12.76; S, 9.74. Found: C, 49.12; H, 4.92; N, 12.62; S, 9.84. IR (KBr): 2960 m, 2920 s, ν(BH) 2530 m, 1540 s, 1440 s, 1430 s, 1410 s, 1370 s, 1200 s, 1100 s, 1060 s, 1030 m, ν(MoO) 950 s, 910 m, 850 m, 810 m, 770 m, 740 m, 700 s, 690 m, 650 m, 560 s, 500 m, 470 m, 350 w, 290 s cm^{-1}. Mass spectrum: *m/z* 658 (85%). Cyclic voltammetry (CH_3CN): $E_{1/2}$ +0.48 V, ΔE_{pp} 65 mV, I_{pa}/I_{pc} 1.05.

***cis*-$LMoO_2(S_2PR_2$-*S*). R = Pr^i. Method 1.** A mixture of $LMoO_2Cl$ (0.5 g, 1.09 mmol) and $NaS_2PPr^i_2$ (0.27 g, 1.3 mmol) was stirred in dichloromethane (35 mL) at 35 °C for 24 h. The resulting mixture was evaporated to dryness and flash chromatographed on silica gel using dichloromethane as the solvent. The main orange fraction was evaporated to dryness to yield the product. Yield: 0.59 g (90%).

Method 2. A toluene (50 mL) solution of $LMoO(S_2PPr^i_2)$ (1.0 g, 1.69 mmol) and dry, deoxygenated dimethyl sulfoxide (1.2 mL, 16.9 mmol) was stirred at 50 °C in a sealed flask for 6 h. After this period the solvent was removed in vacuo and the resultant viscous mixture was heated at 60 °C and 0.01 mmHg pressure for 12 h. The crude gold-yellow product was purified by chromatography using silica gel and dichloromethane as eluent. Yield: 0.89 g (87%).

Anal. Calcd for $C_{21}H_{36}BMoN_6O_2PS_2$: C, 41.59; H, 5.98; N, 13.86; S, 10.57. Found: C, 41.53; H, 6.02; N, 13.90; S, 10.50. IR (KBr): 2950 m, 2910 m, ν(BH) 2525 m, 1530 s, 1440 s, 1410 s, 1355 s, 1200 s, 1060 s, $\nu(MoO_2)$ 930 m & 900 s, 805 m, 699 m, 635 w, 570 w cm^{-1}. Mass spectrum: *m/z* 606 (100%). Cyclic voltammetry (CH_3CN): E_{pc} −0.45 V (irreversible).

R = Ph. A toluene (40 mL) solution of $LMoO(S_2PPh_2)$ (1.46 g, 2.22 mmol) and dry, deoxygenated dimethyl sulfoxide (0.64 mL, 8.8 mmol) was heated at 60 °C in a sealed flask for 6 h. Reduction of the volume by half and cooling of the reaction to ice-salt temperatures afforded the yellow product, which was filtered aerobically and washed with *n*-hexane. The product may be recrystallized from toluene if further purification is required. Yield: 1.1 g (74%).

Anal. Calcd for $C_{27}H_{32}BMoN_6O_2PS_2$: C, 48.08; H, 4.78; N, 12.46; S, 9.51. Found: C, 48.18; H, 4.81; N, 12.36; S, 9.57. Mass spectrum: *m/z* 676 (10%). Cyclic voltammetry (CH_3CN): E_{pc} −0.46 V (irreversible).

Kinetics Studies. Reactions were followed spectrophotometrically using a Shimadzu UV-240 spectrophotometer and quartz cells. Solutions were equilibrated at the specified temperatures prior to use. Pseudo-first-order conditions were employed for each run with [substrate]/[Mo complex] equaling 200/1, 150/1, 100/1, 50/1, and 10/1 for the reduction of Me_2SO by $LMoO(S_2PR_2)$ and 60/1, 42/1, 21/1, and 14/1 for the oxidation of PPh_3 by $LMoO_2(S_2PPr_2)$. The initial concentrations of molybdenum complex were 3.0 and 2.92 mM, respectively. Fresh solutions were prepared on a regular basis.

Results

Syntheses and Characterization. The green oxo−Mo(IV) complexes $LMoO(S_2PR_2)$ were obtained in good yields from the reactions of $MoO(S_2PR_2)_2$ and KL in refluxing toluene. They were highly soluble in chlorinated solvents, slightly soluble in

(23) Trofimenko, S. *J. Am. Chem. Soc.* **1967**, *89*, 6288.
(24) (a) Christen, P. J.; van der Linde, L M.; Hooge, F. N. *Rec. Trav. Chim.* **1959**, *78*, 161. (b) Corbin, J. L.; Newton, W. E. *Org. Prep. Proc. Int.* **1975**, *7*, 309. (c) For R = Me: Cavell, R. G.; Byers, W.; Day, E. D. *Inorg. Chem.* **1971**, *10*, 2710.
(25) Chen, G. J.-J.; McDonald, J. W.; Newton, W. E. *Inorg. Chem.* **1976**, *15*, 2612.
(26) Desbois, M.-H.; Astruc, D. *New J. Chem.* **1989**, *13*, 595.

Table 1. Spectroscopic Data for $LMoO(S_2PR_2)$ and $LMoO_2(S_2PR_2)$ Complexes[a]

compd	ν(MoO) (KBr), cm^{-1}	^1H NMR, δ (multiplicity, no. of H, J in Hz) ($CDCl_3$)		^{31}P NMR, δ ($CDCl_3$)	electronic spectrum λ_{max}, nm (ϵ, $M^{-1}\cdot cm^{-1}$) (CH_2Cl_2)
		$S_2PR_2^-$ ligand	L ligand (all singlets)		
$LMoO(S_2PMe_2)$	960	2.21 (d, 3H, J_{PH} 13), 2.48 (d, 3H, J_{PH} 13)	2.24 (3H), 2.43 (6H), 2.57 (3H), 2.61 (6H), 5.56(1H), 5.94 (2H)		670 (100), 387 (105)
$LMoO(S_2PEt_2)$	960	1.33 (dt, 3H, ^3J 7.5, J_{PH} 20), 1.37 (dt, 3H, ^3J 7.5, J_{PH} 20), 2.3−2.8 (m, 4H)	2.23 (3H), 2.42 (6H), 2.54 (3H), 2.62 (6H), 5.54 (1H), 5.92 (2H)		675 (100), 385 (103)
$LMoO(S_2PPr_2)$	950	1.41 (dd, 6H, ^3J 7.3, J_{PH} 17), 1.45 (dd, 6H, ^3J 7.3, J_{PH} 17), 2.80 and 3.20 (m, 1H)	2.22 (3H), 2.41 (6H), 2.52 (3H), 2.63 (6H), 5.53 (1H), 5.91 (2H)	164.0	677 (108), 404 (90)
$LMoO(S_2PPh_2)$	950	7.3−8.1 (m, 10H)	2.10 (3H), 2.23 (3H), 2.44 (6H), 2.68 (6H), 5.45 (1H), 5.95 (2H)	138.0	670 (125), 420 (sh 250), 380 (510)
$LMoO_2(S_2PPr_2)$	930, 900	1.28 (dd, 6H, ^3J 7, J_{PH} 19), 1.30 (dd, 6H, ^3J 7, J_{PH} 19), 2.4−2.7 (m, 2H)	2.34 (3H), 2.37 (6H), 2.50 (3H), 2.62 (6H), 5.83 (3H)	80.0	450 (sh 340), 350 (sh 2200)
$LMoO_2(S_2PPh_2)$	930, 900	7.4−8.1 (m, 10H)	2.32 (3H), 2.35 (6H), 2.45 (6H), 2.48 (3H), 5.08 (2H), 5.82 (1H)	65.0	450 (sh 480), 340 (sh 5420)

[a] Complete listings of infrared and mass spectral data are given in the Experimental Section.

benzene and toluene, but virtually insoluble in hydrocarbons, ethers, and alcohols. All underwent slow air oxidation in solution, but only the methyl derivative was air-sensitive (slightly) in the solid state. Oxidation of $LMoO(S_2PPr_2)$ and $LMoO(S_2PPh_2)$ by Me_2SO in toluene produced high yields of $LMoO_2(S_2PPr_2)$ and $LMoO_2(S_2PPh_2)$, respectively. These complexes were also formed in the reactions of $LMoO_2Cl$ with NaS_2PR_2. Both compounds were decomposed by air or prolonged contact with silica gel and were stored under dinitrogen.

Microanalytical, mass spectrometric and electrochemical results (Experimental Section) and spectroscopic data (Table 1) were consistent with the proposed formulations. A medium intensity B−H stretch (ca. 2525 cm^{-1}) and characteristic fingerprint bands confirmed the presence of the L and $S_2PR_2^-$ ligands. The $LMoO(S_2PR_2)$ complexes exhibited strong ν(Mo═O) bands at 960 cm^{-1} while the $LMoO_2(S_2PR_2)$ complexes were characterized by two strong bands at *ca.* 930 and 900 cm^{-1}, assigned to $\nu_s(MoO_2)$ and $\nu_{as}(MoO_2)$ stretching modes, respectively. An absorption of medium intensity at ca. 530 cm^{-1} was assigned to the ν(P═S) mode of the monodentate dithiophosphinate ligands of $LMoO_2(S_2PR_2)$. The ^1H NMR spectra of the complexes were consistent with molecular C_s symmetry in solution. In the alkyl derivatives, coupling of the methyl protons to the ^{31}P nucleus (J_{HP} 13−20 Hz) was observed. The L ligand in each complex was characterized by two methine resonances (1:2 intensity ratio) and four methyl resonances (3:3:6:6 intensity ratio). The two methine resonances of the $LMoO(S_2PR_2)$ complexes were separated by ca. 0.4 ppm while, in common with related dioxo−Mo(VI) and −W(VI) complexes,[13,27] those of $LMoO_2(S_2PR_2)$ exhibited virtually identical chemical shifts. The $LMoO(S_2PR_2)$ complexes exhibited ^{31}P NMR resonances in the range from δ 138 to δ 164, whereas $LMoO_2(S_2PR_2)$ exhibited relatively shielded resonances at δ 65 and δ 80. The ^{31}P resonances of the isopropyl derivatives were consistently deshielded relative to their phenyl analogues and in all cases the resonances were considerably deshielded relative to that of free HS_2PR_2 (ca. δ 60). The electronic spectra of $LMoO(S_2PR_2)$ exhibited two d−d absorption bands at ca. 670 nm (ϵ 100−125 $M^{-1}\cdot cm^{-1}$) and 380−405 nm (ϵ 90−510 $M^{-1}\cdot cm^{-1}$). The electronic spectra of $LMoO_2(S_2PR_2)$ exhibited only UV LMCT bands with very weak shoulders tailing into the visible region. The $LMoO(S_2PR_2)$ complexes were reversibly electrochemically oxidized at potentials in the range 0.40−0.48 V vs SCE. The $LMoO_2(S_2PR_2)$ complexes exhibited irreversible reduction processes in electrochemical experiments. We were unable to grow single crystals suitable for X-ray diffraction studies.

Kinetics Studies. The kinetics of reactions 5 and 6 were investigated in toluene solution under pseudo-first-order conditions (C_5H_5NO = pyridine *N*-oxide).[28] Disappearance of the ca. 677 nm band of $LMoO(S_2PR_2)$ was used to monitor each reaction and tight isosbestic points, consistent with two-component reactions, were obtained in all cases (see Figure 1). The reactions were first-order with respect to molybdenum complex as plots of $\ln(A_t/A_o)$ vs time were linear to at least 90% reaction completion. The reactions were also first-order in substrate (Me_2SO or C_5H_5NO) as shown by linear plots of k_{obs} vs $[substrate]_o$ (see Figure 2). Therefore, the second-order rate law defined in eq 7 pertained to the oxidation of $LMoO(S_2PR_2)$ by both Me_2SO and C_5H_5NO. Second-order rate constants, k, are summarized in Table 2. Plots of $\ln k$ vs T^{-1} permitted the calculation of the thermodynamic parameters given in Table 2. The second-order rate constants for eq 5 depended on R in the order Me < Et < Pr. The corresponding trends for $\Delta H^{\ddagger}$ (Me > Et > Pr) and $\Delta S^{\ddagger}$ (Me > Et > Pr) lead to a similar dependence on R for $\Delta G^{\ddagger}$.

$$LMoO(S_2PR_2) + Me_2SO \rightarrow LMoO_2(S_2PR_2) + Me_2S \quad (5)$$

$$LMoO(S_2PPr_2) + C_5H_5NO \rightarrow LMoO_2(S_2PPr_2) + C_5H_5N \quad (6)$$

$$-d[LMoO(S_2PR_2)]/dt = k[LMoO(S_2PR_2)][substrate] \quad (7)$$

The reactions of $LMoO(S_2PR_2)$ with $NBu^n_4NO_3$ were clean and rapid and produced high, isolable yields of $LMoO_2(S_2PR_2)$. In situ, these were eventually decomposed by the NO_2^- produced in the reaction but addition of sulfamic acid, a scavenger of NO_2^-, effectively prevented this decomposition.

(27) (a) Roberts, S. A.; Young, C. G.; Kipke, C. A.; Cleland, W. E., Jr.; Yamanouchi, K.; Carducci, M. D.; Enemark, J. H. *Inorg. Chem.* **1990**, *29*, 3650. (b) Eagle A. A.; Young, C. G.; Tiekink, E. R. T. *Organometallics*, **1992**, *11*, 2934.

(28) Wilkins, R. G. *Kinetics and Mechanism of Reactions of Transition Metal Complexes*, 2nd ed.; VCH: New York, 1991, pp 5−13, 87−89, 154−158.

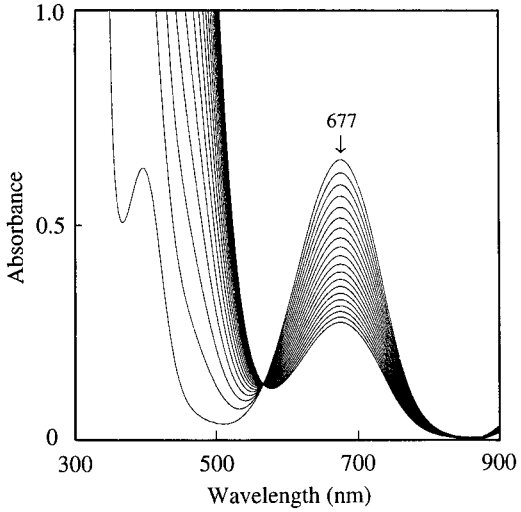

Figure 1. Spectral changes in the reaction of $LMoO(S_2PPr_2)$ with Me_2SO (1:100, $[Me_2SO]_o = 0.6$ M) at 25 °C in toluene. The spectra were recorded at time intervals of 20 min.

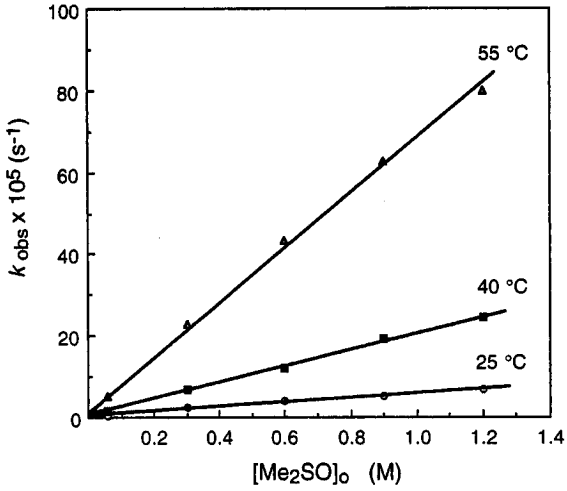

Figure 2. Plots of k_{obs} vs $[Me_2SO]_o$ for the reaction of $LMoO(S_2PPr_2)$ and Me_2SO.

Kinetics studies were precluded by the solvent incompatibility of the molybdenum complexes and sulfamic acid.

The reactions of $LMoO_2(S_2PR_2)$ with PPh_3, in dry toluene and on synthetic scales, produced high yields of $LMoO(S_2PR_2)$ according to eq 8. At low concentrations and moderate

$$LMoO_2(S_2PR_2) + PPh_3 \rightarrow LMoO(S_2PR_2) + OPPh_3 \quad (8)$$

temperature extremes, this reaction was accompanied by a number of side reactions; meaningful kinetics studies were possible only for the reaction of $LMoO_2(S_2PPr_2)$ and PPh_3 at 30 °C. In these studies, the formation of $LMoO(S_2PPr_2)$ was monitored spectrophotometrically by growth of the band at 677 nm. The reaction was zero-order with respect to $LMoO(S_2PPr_2)$. Plots of $C_t - C_o$ [for $LMoO(S_2PPr_2)$] vs time were linear indicating that the rate determining step occurs prior to the formation of $LMoO(S_2PPr_2)$. The pseudo-zero-order rate constants, k_{obs}, were used to show first-order dependence in $LMoO_2(S_2PPr_2)$ as well as PPh_3, giving the rate law shown in equation 9.[28] The overall second-order rate constant for the

$$d[LMoO(S_2PPr_2)]/dt = k[LMoO_2(S_2PPr_2)][PPh_3] \quad (9)$$

reaction was $k = 2.5(3) \times 10^{-4}$ $M^{-1}\cdot s^{-1}$. In reactions monitored by integrated ^{31}P NMR spectroscopy, $LMoO(S_2PPr_2)$ and $LMoO_2(S_2PPr_2)$ were independently observed to catalyze the oxidation of PPh_3 by Me_2SO at turnover rates of ca. 0.9 mol of PPh_3/(mol of catalyst/h).

Generation of Mo(V) Complexes. A number of mononuclear, EPR-active Mo(V) species were generated; EPR data and assignments are summarized in Table 3. Addition of a 10-fold excess of NBu^n_4SH in tetrahydrofuran (THF)/CH_3CN (9:1) to yellow THF solutions of $LMoO_2(S_2PPr_2)$ resulted in the immediate formation of a yellow-green solution. The species formed exhibited a broad ($W_{1/2}$ 25 G) EPR signal with a very low isotropic g value of 1.921. The first frozen-glass EPR spectrum was highly anisotropic with g_1, g_2, and g_3 values of 1.997, 1.932, and 1.837, respectively (Figure 3a); the room and low-temperature spectra were consistent with generation of the dioxo−Mo(V) anion, $[LMoO_2(S_2PPr^i_2\text{-}S)]^-$.[20−22] With time, the initial signal was replaced by another broad isotropic solution (g 1.938) and anisotropic frozen-glass EPR signal (Figure 3b), with g_1, g_2, and g_3 values of 2.013, 1.933, and 1.880, respectively. This very persistent signal was assigned to the oxothio−Mo(V) anion, $[LMoOS(S_2PPr^i_2\text{-}S)]^-$.[20,21] The EPR spectra generated upon reaction of $LMoO_2(S_2PPh_2)$ and NBu^n_4SH were consistent with the formation of the analogous dioxo− and oxothio−Mo(V) anions. There was no evidence for the generation of $[Mo^VS_2]^+$ species even after extended incubation of the reaction mixtures. The EPR signals of the Mo(V) species rapidly disappeared upon admission of dioxygen. The following experiments were performed on a small synthetic scale, and the

Table 2. Kinetic and Thermodynamic Data for the Reactions of $LMoO(S_2PR_2)$ with Me_2SO and C_5H_5NO in Toluene[a]

compd	temp, °C	k, $M^{-1}\cdot s^{-1}$	$\Delta H^{\ddagger}$, $kJ\cdot mol^{-1}$	$\Delta S^{\ddagger}$, $J\cdot K^{-1}\cdot mol^{-1}$	$\Delta G^{\ddagger}$,[b] $kJ\cdot mol^{-1}$
$LMoO(S_2PMe_2)$	25	$2.1(1) \times 10^{-5}$			
	40	$9.0(1) \times 10^{-5}$	73(1)	−88(1)	100(2)
	55	$3.39(2) \times 10^{-4}$			
$LMoO(S_2PEt_2)$	25	$3.6(1) \times 10^{-5}$			
	40	$1.36(3) \times 10^{-4}$	68(1)	−99(2)	99(2)
	55	$4.98(1) \times 10^{-4}$			
$LMoO(S_2PPr_2)$	25	$5.5(3) \times 10^{-5}$			
	40	$2.08(5) \times 10^{-4}$	63(1)	−111(1)	98(2)
	55	$6.83(1) \times 10^{-4}$			
$LMoO(S_2PPr_2)$*	25	$4.80(3) \times 10^{-4}$			
	40	$1.54(5) \times 10^{-3}$	62(1)	−90(1)	90(1)
	55	$3.55(6) \times 10^{-3}$			
$LMoO\{S_2P(OEt)_2\}$[13]	25	$1.51(6) \times 10^{-5}$			
	40	$5.46(6) \times 10^{-5}$	64(2)	−121(3)	102.8
	55	$1.73(2) \times 10^{-4}$			

[a] Data for reaction of $LMoO(S_2PPr_2)$ and C_5H_5NO are indicated by an asterisk in the compound listing. All other data pertain to reactions involving Mo complex and Me_2SO. [b] Calculated at 40 °C.

Table 3. EPR Parameters for the Mo(V) Complexes[a]

complex	g_{av} ($W_{1/2}$, G)	g_1	g_2	g_3	$a(^1H)$	$a(^{31}P)$	$a(^{95,97}Mo)$
$[LMoO_2(S_2PPr_2)]^-$	1.921 (24)						61.8
$[LMoO_2(S_2PPh_2)]^-$	1.919 (25)						63.1
$[LMoO_2(SPh)]^-$ [b,c]	1.920 (20)						41.4
$[LMoO_2(S_2PPr_2)]^-$	1.922	1.997	1.932	1.837			A_1 28.6; A_3 71.2
$[LMoO_2(S_2PPh_2)]^-$	1.921	1.996	1.931	1.835			A_1 30.9; A_3 74.5
$[LMoO_2(SPh)]^-$ [b,c]	1.920	1.992	1.931	1.839			A_1 27.9; A_3 67.9
$[(L\text{-}N_2S_2)MoO_2]^-$ [d]	1.904	1.987	1.916	1.811			A_1 27.1; A_3 68.8
$[LMoOS(S_2PPr_2)]^-$	1.938 (18)						43.5
$[LMoOS(S_2PPh_2)]^-$	1.934 (15)						43.5
$[LMoOS(SCH_2Ph)]^-$ [c]	1.954 (18)						34.1
$[LMoOS(S_2PPr_2)]^-$	1.941	2.013	1.933	1.880			A_1 43.4
$[LMoOS(S_2PPh_2)]^-$	1.939	2.012	1.932	1.877			A_1 43.5
$[LMoOS(SCH_2Ph)]^-$ [c]	1.954	2.022	1.948	1.898			
$[(L\text{-}N_2S_2)MoOS]^-$ [d]	1.946	2.016	1.934	1.888			A_1 22.6; A_3 53.5
$[LMoO(S_2PMe_2)]^+$	1.964					40.8	41.5
$[LMoO(S_2PEt_2)]^+$	1.962					37.6	41.6
$[LMoO(S_2PPr_2)]^+$	1.964					34.4	41.7
$[LMoO(S_2PPh_2)]^+$	1.963					41.6	41.4
$LMoO(OH)(S_2PMe_2)$	1.949				12.2	12.2	45.5
$LMoO(OH)(S_2PEt_2)$	1.950				12.2	12.3	45.3
$LMoO(OH)(S_2PPr_2)$	1.950				12.3	12.3	45.3
$LMoO(OH)(S_2PPh_2)$	1.949				12.0	12.0	45.8
$LMoO(OH)(SPh)$[c]	1.951				11.5		42.9
$(L\text{-}N_2S_2)MoO(OH)$[d]	1.957	1.981	1.947	1.944	15.1		

[a] Conditions and solvents are described in the text. The first frozen-glass spectra of $[LMoO_2(S_2PR_2)]^-$ were obtained on samples frozen within 5 s of mixing. Isotropic data were obtained from solution spectra at room temperature; anisotropic data were obtained from frozen-glass samples at 77 K. Units of $a = 10^{-4}$ cm^{-1}. [b] Data from ref 22. [c] Data from ref 21. [d] Data from ref 20.

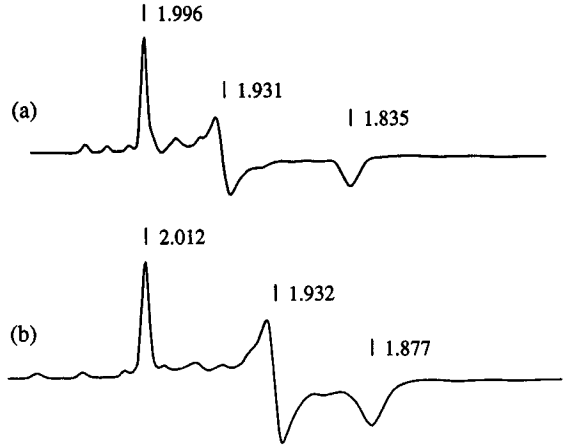

Figure 3. Frozen-glass EPR spectra of complexes generated upon reaction of $LMoO_2(S_2PPh_2)$ with NBu^n_4SH in THF/MeCN: (a) $[LMoO_2(S_2PPh_2)]^-$; (b) $[LMoOS(S_2PPh_2)]^-$.

products were isolated as a combined fraction using flash chromatography and then identified and quantified by ^{1}H NMR spectroscopy: Reaction of *in situ* generated $[LMoOS(S_2PPr_2)]^-$ with carefully dried dioxygen resulted in the formation of the oxothio−Mo(VI) complex $LMoOS(S_2PPr_2\text{-}S)$[29] and $LMoO_2(S_2PPr_2)$, in yields of 90% and 10%, respectively: When the dioxygen was not dried, the same species were formed but the yields were 20% and 80%, respectively.

In the presence of water (3−5 M), reactions of $LMoO_2(S_2PR_2)$ with PPh_3 in THF produced species which exhibited characteristic three-line EPR spectra (ca. g 1.95, $a(^1H)$ 12 × 10^{-4} cm^{-1}, $a(^{31}P)$ 12 × 10^{-4} cm^{-1}, and $a(^{95,97}Mo)$ 45 × 10^{-4} cm^{-1}; see Figure 4a). These were the only EPR-active species formed and their signal intensity reached a maximum when Mo:$PPh_3 \leq 0.5$. They were moderately stable and persisted in solution for several hours. Weaker, less-persistent EPR signals were produced when lower water concentrations were employed.

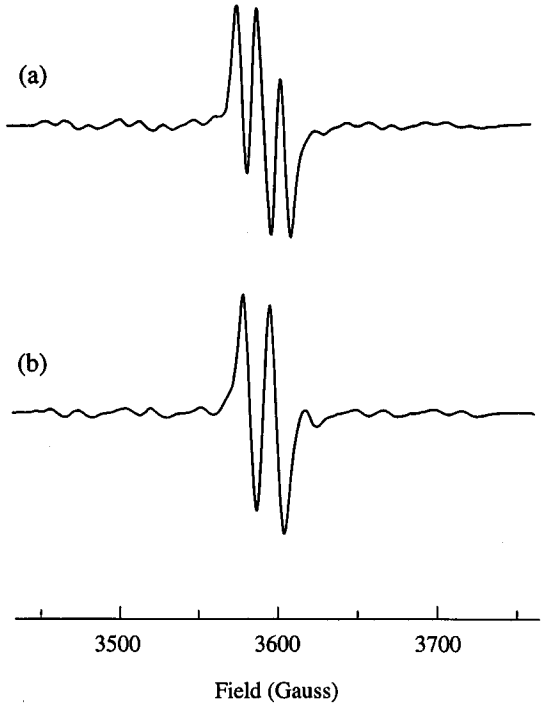

Figure 4. Solution EPR spectra of complexes generated upon reaction of $LMoO_2(S_2PPr_2)$ with excess PPh_3 in 3−5 M ^nH_2O in THF: (a) $LMoO(OH)(S_2PPr_2)$; (b) $LMoO(OD)(S_2PPr_2)$.

In the presence of D_2O (3−5 M in THF), reactions of $LMoO_2(S_2PR_2)$ with PPh_3 produced species which exhibited two-line EPR spectra (ca. g 1.95, $a(^{31}P)$ 12 × 10^{-4} cm^{-1}, and $a(^{95,97}Mo)$ 45 × 10^{-4} cm^{-1}; see Figure 4b). The signals were assigned to the (hydroxo)oxo−Mo(V) complexes, $LMoO(OH)(S_2PR_2\text{-}S)$, and the deuterated analogues.

Oxidation of $LMoO(S_2PR_2)$ was reversible on the cyclic voltammetric time scale and the addition of sub-stoichiometric quantities of $[FeCp_2]PF_6$ in THF/CH_3CN (7:1) to THF solutions of $LMoO(S_2PR_2)$ (final Fe:Mo 1:19) resulted in orange-brown solutions which exhibited characteristic doublet EPR signals

(29) Eagle, A. A.; Laughlin, L. J.; Young, C. G.; Tiekink, E. R. T. *J. Am. Chem. Soc.* **1992**, *114*, 9195.

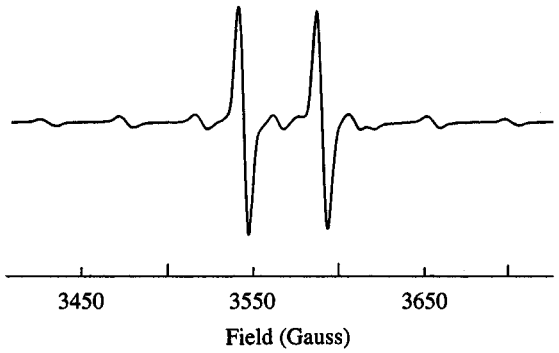

Figure 5. Solution EPR spectrum of $[LMoO(S_2PPr_2)]^+$.

with g ca. 1.963 and $a(^{31}P)$ 34.4 × 10^{-4} to 41.6 × 10^{-4} cm^{-1} (Figure 5). The $^{95,97}Mo$ hyperfine features were also split into doublets. The signals were assigned to the oxo−Mo(V) cations $[LMoO(S_2PR_2\text{-}S,S')]^+$. The addition of deoxygenated water to solutions of the cationic complexes resulted in the generation of species which exhibited triplet EPR signals identical to those observed in the reactions of $LMoO_2(S_2PR_2)$ with PPh_3 in wet THF; again, the (hydroxo)oxo−Mo(V) species were stable for several hours under anaerobic conditions but reacted rapidly with dioxygen to produce $LMoO_2(S_2PR_2)$ (identified by ^1H NMR spectroscopy). Addition of deoxygenated D_2O to solutions of $[LMoO(S_2PR_2)]^+$ resulted in the generation of species which exhibited doublet EPR signals assigned to the deuterated species $LMoO(OD)(S_2PR_2\text{-}S)$. Addition of $[FeCp_2]PF_6$ to solutions of $LMoO(S_2PR_2)$ in 3−5 M water/THF produced $LMoO(OH)(S_2PR_2)$ without the detection of $[LMoO(S_2PR_2)]^+$.

Discussion

A well established methodology[13,30] was adopted for the synthesis of the $LMoO(S_2PR_2)$ complexes (eq 10 or 11, coupled with eq 12). The $LMoO_2(S_2PR_2)$ complexes may be prepared

$$MoO_2(S_2PR_2)_2 + PPh_3 \rightarrow MoO(S_2PR_2)_2 + OPPh_3 \quad (10)$$

$$Mo_2O_3(S_2PMe_2)_4 + PPh_3 \rightarrow 2MoO(S_2PMe_2)_2 + OPPh_3 \quad (11)$$

$$MoO(S_2PR_2)_2 + KL \rightarrow LMoO(S_2PR_2) + KS_2PR_2 \quad (12)$$

by metathesis reactions or via OAT to $LMoO(S_2PR_2)$ (eqs 5 and 6); reactions involving the biologically important substrates Me_2SO, pyridine *N*-oxide, and NO_3^- may be exploited in these syntheses. The physical and spectroscopic data are entirely consistent with the proposed formulations. The structures of $LMoO(S_2PR_2)$ and $LMoO_2(S_2PR_2)$ are expected to be analogous to those of the respective dithiophosphate complexes, $LMoO\{S_2P(OEt)_2\text{-}S,S'\}$ and *cis*-$LMoO_2\{S_2P(OEt)_2\text{-}S\}$,[13] which exhibit six-coordinate, distorted octahedral structures comprising facial L, ambidentate $S_2PR_2^-$, and terminal oxo ligands. In the dioxo complex, the monodentate dithio ligand adopts an extended configuration in which the uncoordinated sulfur is well removed from the molybdenum center [Mo···S(2) = 5.42 Å].[13]

Detailed kinetics studies of selected OAT reactions (eqs 5, 6 and 8) have been undertaken. For OAT to $LMoO(S_2PR_2)$, associative mechanisms are consistent with the second-order rate laws and large negative $\Delta S^\ddagger$ values. Although associative mechanisms imply the coordination of the substrate to molybdenum during the transition state it is unlikely on steric grounds that seven-coordinate intermediates are formed. It is more likely that cleavage of an Mo−S bond is initiated by close approach and binding of the substrate, a step followed by rapid OAT to produce $LMoO_2(S_2PR_2)$ and reduced substrate. This appears to be a general mechanism for atom transfer reactions involving related oxo−[31,32] and thio−Mo(IV)[33] complexes.

The OAT reaction of $LMoO(S_2PPr_2)$ with pyridine *N*-oxide is nearly an order of magnitude faster than that between $LMoO(S_2PPr_2)$ and Me_2SO. The significantly different X−O bond dissociation energies[34] of pyridine *N*-oxide (D_{N-O} 301 kJ·mol^{-1}) and Me_2SO (D_{S-O} 364 kJ·mol^{-1}) are expected to contribute to the observed rate difference through the enthalpy terms. However, it is principally the entropy term which dictates the faster rate for the pyridine *N*-oxide reaction. Although the oxo−Mo(IV) complexes are capable of reducing NO_3^- to NO_2^-, experimental limitations precluded detailed kinetics studies of this important biologically-relevant reaction.

The reaction in eq 13 has also been subject to kinetics studies;[13] comparative data are included in Table 2. Here too,

$$LMoO\{S_2P(OEt)_2\} + Me_2SO \rightarrow LMoO_2\{S_2P(OEt)_2\} + Me_2S \quad (13)$$

the sizable negative $\Delta S^\ddagger$ and the second-order rate law implicate an associative mechanism with the binding of Me_2SO to the Mo complex in the transition state. This reaction is slower than any involving the dithiophosphinate complexes (eq 5). However, related reactions are generally faster than those reported herein.[2,8] The reaction of $MoO(S_2CNEt_2)_2$ with Me_2SO in 1,2-dichloroethane at 25 °C is second-order with $k = 1.6(1) \times 10^{-4}$ $M^{-1}\cdot s^{-1}$. The reactions of $(L\text{-}NS_2)MoO(DMF)$ with Me_2SO and a variety of other *S*- and *N*-oxides exhibit saturation kinetics postulated to arise from complexation of substrate to unsaturated $(L\text{-}NS_2)MoO$ prior to product formation. The reaction of $(L\text{-}NS_2)MoO(DMF)$ with Me_2SO in DMF at 23 °C has a maximum reaction velocity of $k_1 = 1.50(3) \times 10^{-3}$ s^{-1}. In contrast, the reaction of $(L\text{-}NS)_2MoO$ with Me_2SO is second-order with $k = 1.01(2) \times 10^{-4}$ $M^{-1}\cdot s^{-1}$.[12a]

Second-order kinetics characterize all other previously examined reactions involving phosphines and dioxo−Mo(VI) complexes.[2] The reaction of $MoO_2(S_2CNEt_2)_2$ and PPh_3 in 1,2-dichloroethane is the fastest for which kinetics data are available, with $k = 7.1(3) \times 10^{-2}$ $M^{-1}\cdot s^{-1}$. The reaction of $(L\text{-}NS_2)MoO_2$ with PPh_3 in DMF is characterized by a rate constant $k = 7(1) \times 10^{-3}$ $M^{-1}\cdot s^{-1}$. The reaction of $LMoO_2(S_2PPr_2)$ and PPh_3 is slower than the above reactions and the reactions of both $LMoO_2\{S_2P(OEt)_2\}$[13] and $LMoO_2(SPh)$[28] with PPh_3 (k = 3.4(1) x 10^{-3} and 5.9(2) × 10^{-4} $M^{-1}\cdot s^{-1}$, respectively, at 25 °C). An associative mechanism is implicated by the second-order kinetics of these reactions.

The complexes generated when $LMoO_2(S_2PR_2)$ are reduced by NBu^n_4SH exhibit broad isotropic solution EPR spectra and highly anisotropic frozen-glass EPR spectra, with g and A values

(30) Young, C. G.; Roberts, S. A.; Ortega, R. B.; Enemark, J. H. *J. Am. Chem. Soc.* **1987**, *109*, 2938.

(31) Laughlin, L. J. Ph.D. Dissertation, University of Melbourne, Australia, 1993.

(32) Sulfur atom transfer from propylene sulfide to $LMoO(S_2PPr_2)$ in toluene obeys the second-order rate law $-d[LMoO(S_2PPr_2)]/dt = k[LMoO(S_2PPr_2)][C_3H_6S]$ with $k = 7.0(1) \times 10^{-6}$ $M^{-1}\cdot s^{-1}$ at 35 °C. The activation parameters for this reaction are $\Delta H^\ddagger = 61(1)$ kJ·mol^{-1}, $\Delta S^\ddagger = -142(2)$ J·K^{-1}·mol^{-1} and $\Delta G^\ddagger = 106(2)$ kJ·mol^{-1} (at 35 °C).

(33) Reaction of $LMoS(S_2PR_2\text{-}S,S')$ (L = hydrobis(3-isopropylpyrazol-1-yl)(5-isopropylpyrazol-1-yl)borate] with pyridine *N*-oxide results in the formation of $LMoOS(S_2PR_2\text{-}S)$. The reaction is the only example of the generation of an oxothio−Mo(VI) complex via clean oxygen atom transfer to a thio−Mo(IV) complex. Laughlin, L. J.; Colmanet, S.; Scrofani, S. D. B.; Young, C. G. Unpublished results.

(34) Holm, R. H.; Donahue, J. P. *Polyhedron* **1993**, *12*, 571.

characteristic of $[Mo^{V}O_2]^+$ centers.[20−22] As well as acting as reductant, hydrosulfide provides the highly basic conditions which protect $[LMoO_2(S_2PR_2)]^-$ from protonation. The stability of $[LMoO_2(S_2PR_2)]^-$ under these conditions contrasts with the irreversible behavior observed upon electrochemical reduction of $LMoO_2(S_2PR_2)$. Similar chemistry was employed by Spence and Wedd and co-workers to generate $[(L\text{-}N_2S_2)Mo^{V}O_2]^-$ [L-N_2S_2 = dianion of *N*,*N*′-dimethyl-*N*,*N*′-bis(2-sulfanylphenyl)-ethylenediamine], which also exhibits a highly anisotropic EPR spectrum (Table 3).[20] A range of closely related $[LMoO_2X]^-$ [L = hydrotris(3,5-dimethylpyrazol-1-yl)borate, hydrotris(3-isopropylpyrazol-1-yl)borate, hydrotris(3,5-dimethyl-1,2,4-triazol-1-yl)borate; X = Cl, Br, OMe, OR, SR] complexes have been produced by electrochemical[21] or chemical (SH^-,[21] $CoCp_2$[22]) reduction of $LMoO_2X$. Cobaltocene reduction of $LMoO_2(SPh)$ permits the isolation of crystalline $[CoCp_2]$-$[LMoO_2(SPh)]$ salts which have been extensively characterized by spectroscopic and X-ray diffraction methods.[22] Like the $[LMoO_2(S_2PR_2)]^-$ complexes under discussion, all these $[LMoO_2X]^-$ complexes exhibit characteristic, highly anisotropic EPR spectra (selected examples given in Table 3).

The dioxo−Mo(V) complexes are slowly converted to oxothio−Mo(V) complexes, $[LMoOS(S_2PR_2)]^-$, in the presence of excess SH^-. The π^* nature of the singly occupied molecular orbital of the $[MoO_2]^+$ fragment[21,22] weakens the Mo−O bonds and facilitates the substitution of an oxo ligand. The highly basic SH^- medium stabilizes and permits the observation of the oxothio complexes. Similarly, $[(L\text{-}N_2S_2)MoO_2]^-$ and a number of other $[LMoO_2X]^-$ complexes are converted to oxothio−Mo(V) complexes by excess SH^-.[20,21] The oxothio−Mo(V) complexes exhibit anisotropic spectra with higher *g* values and lower *A* values than the corresponding dioxo−Mo(V) complexes, consistent with previous observations.[35] Strong supporting evidence for an oxothio−Mo(V) formulation is the generation of $[LMoOS(S_2PR_2)]^-$ upon cobaltocene reduction of $LMoOS(S_2PR_2)$[31] and the regeneration of $LMoOS(S_2PR_2)$ upon air oxidation of $[LMoOS(S_2PR_2)]^-$ (vide infra).

The above EPR signals are rapidly lost upon admission of dioxygen. Oxidation of $[LMoO_2(S_2PR_2)]^-$ produces $LMoO_2(S_2PR_2)$, while oxidation of $[LMoOS(S_2PR_2)]^-$ under anhydrous conditions produces oxothio−Mo(VI) complexes, $LMoOS(S_2PR_2)$. In the presence of water, oxidation of $[LMoOS(S_2PR_2)]^-$ produces significant quantities of $LMoO_2(S_2PR_2)$ and only small amounts of $LMoOS(S_2PR_2)$. The effect of water on the oxidation of $[LMoOS(S_2PR_2)]^-$ may be rationalized in terms of competing hydrolysis and oxidation reactions. Hydrolysis prior to oxidation would produce $LMoO_2(S_2PR_2)$ and would be enhanced when the reaction is performed using wet dioxygen. The use of carefully dried dioxygen ensures oxidation takes place before hydrolysis, ensuring high yields of $LMoOS(S_2PR_2)$. Adventitious water may account for the partial formation of $LMoO_2(S_2PR_2)$, although superoxide or peroxide species may also be responsible for oxygenation of the molybdenum center. In previous work[20a,b] it was not possible to isolate or detect the putative oxothio−Mo(VI) species formed by oxidation of *in situ* generated $[(L\text{-}N_2S_2)Mo^{V}OS]^-$. The steric protection of L and the unique intramolecular stabilization of the Mo=S unit of $LMoOS(S_2PR_2)$ permit this, the first, demonstration of a $[Mo^{V}OS]^+$ to $[Mo^{VI}OS]^{2+}$ conversion reaction. These observations show that it is possible to generate an oxothio−Mo(VI) center after oxo-by-thio exchange has been executed at a lower oxidation level, in this case Mo(V). Wahl and Rajagopalan postulated oxo-by-thio ligand exchange at Mo(IV) to account for the reactivation of desulfo xanthine oxidase, xanthine dehydrogenase, and aldehyde oxidase, by sulfide and reducing agents.[38] Our work and previous work by Wedd et al.[20] show that reduction to Mo(V) is sufficient to facilitate oxo-by-thio ligand exchange. Importantly, we have now demonstrated the possibility of oxidizing a reduced oxothio species to an oxothio−Mo(VI) species as required by the mechanism proposed by Wahl and Rajagopalan.

On a preparative scale, and in dry solvents, reaction of $LMoO_2(S_2PR_2)$ with PPh_3 proceeds according to eq 8. However, at lower Mo concentrations and in wet solvents, CEPT and CENT reactions lead to the formation of mononuclear, EPR-active Mo(V) complexes. Reaction of $LMoO_2(S_2PR_2)$ with PPh_3 in 3−5 M H_2O/THF resulted in the generation of $LMoO(OH)(S_2PR_2)$. The triplet EPR spectra are consistent with this formulation and with equivalent superhyperfine coupling to a single proton and a single ^{31}P nucleus.[39] Related species exhibit similar EPR spectra (Table 3).[20−22] We propose that the (hydroxo)-oxo−Mo(V) species are formed upon oxidation [by Mo(VI), $LMoO_2(S_2PR_2)$] of a putative (aqua)oxo−Mo(IV) complex, $LMoO(OH_2)(S_2PR_2\text{-}S)$, formed immediately upon OAT to PPh_3: see eq 14 followed by eq 15, giving the overall reaction shown in eq 16 (N- and S-donor ligands excluded for clarity).

$$[Mo^{IV}O_2]^{2+} + PPh_3 + H_2O \rightarrow [Mo^{IV}O(H_2O)]^{2+} + OPPh_3 \quad (14)$$

$$[Mo^{IV}O(H_2O)]^{2+} + [Mo^{VI}O_2]^{2+} \rightarrow 2[Mo^{V}O(OH)]^{2+} \quad (15)$$

$$2[Mo^{VI}O_2]^{2+} + PPh_3 + H_2O \rightarrow 2[Mo^{V}O(OH)]^{2+} + OPPh_3 \quad (16)$$

The large separation of the Mo and uncoordinated dithiophosphinate sulfur is expected to facilitate the binding of water prior to chelation at the vacant site generated by OAT. Related pyridine and acetonitrile solvate complexes are resistant to oxidation and have actually been isolated.[21,27a] The $LMoO(OH)(S_2PR_2)$ complexes are also formed upon addition of water to solutions of $[LMoO(S_2PR_2)]^+$ generated by ferrocenium oxidation of $LMoO(S_2PR_2)$. In both experiments, the presence of D_2O results in the formation of $LMoO(OD)(S_2PR_2)$ which exhibit a doublet EPR signal due solely to superhyperfine coupling to one ^{31}P nucleus; this is consistent with the presence of only one exchangeable proton and the (hydroxo)oxo formulation. The superhyperfine coupling to ^{31}P is dictated by the location of the nucleus relative to the magnetic orbital.[13,40] Chelation of $S_2PR_2^-$ ligands to Mo(V) centers permits favorable orbital overlap, leading to large ^{31}P superhyperfine coupling

(35) An increase in the coordination-sphere sulfur content of oxo−Mo(V) complexes is invariably associated with an increase in the *g* value of the complex. However, it is important to note that the "higher sulfur content, higher *g* value" rule breaks down when oxo ligands are replaced by thio ligands, e.g. in the series $LMoECl_2$[36] and $[LMoE(S_2PR_2)]^+$[37] (E = O, S).

(36) Young, C. G.; Enemark, J. H.; Collison, D.; Mabbs, F. E. *Inorg. Chem.* **1987**, *26*, 2925.

(37) The $[LMoE(S_2PR_2)]^+$ [L = hydrobis(3-isopropylpyrazol-1-yl)(5-isopropylpyrazol-1-yl)borate] complexes were generated by ferrocenium oxidation of the corresponding Mo(IV) complexes. The thio−Mo(V) complexes have lower isotropic *g* values than their oxo analogues (1.961 vs 1.963 for E = S and E = O, respectively, when R = Pr^i). See ref 31.

(38) Wahl, R. C.; Rajagopalan, K. V. *J. Biol. Chem.* **1982**, *257*, 1354.

(39) The analogous dithiocarbamate complexes $[LMoO(S_2CNR_2)]^+$ exhibit singlet EPR signals and do not react with water to form (hydroxo)-oxo species. The (hydroxo)oxo species $LMoO(OH)(C_5H_4NS)$ exhibits a doublet EPR signal (*g* 1.950, $a(^1H) = 10.4 \times 10^{-4}$ cm^{-1}) while the deuterated analogue exhibits a singlet signal. These observations support the presence of superhyperfine coupling to ^{31}P for the dithiophosphinate complexes.

constants, as observed for $[LMoO(S_2PR_2)]^+$ and some dithiophosphate analogues.[13] The monodentate coordination of $S_2PR_2^-$ in $LMoO(OH)(S_2PR_2)$ separates the Mo and P centers and reduces orbital overlap, with consequent reduction of the superhyperfine coupling. Interestingly, $LMoO(OH)(S_2PR_2)$ complexes are produced upon cyanolysis of $LMoOS(S_2PR_2)$ in wet solvents but not in reactions with PPh_3.[41] In dry solvents, the coordinatively unsaturated intermediate formed upon OAT is stabilized by chelation of $S_2PR_2^-$. A degree of lability of the Mo-S bonds in $[LMoO(S_2PR_2)]^+$ is consistent with the formation of $LMoO(OH)(S_2PR_2)$ upon reaction with water. Addition of water to coordinately unsaturated $[LMoO(S_2PPr^i_2)]^+$ [L = dihydrobis(3,5-dimethylpyrazol-1-yl)borate] resulted in decomposition without the formation of mononuclear Mo(V) species;[42] coordinative saturation in the hydrotris(3,5-dimethylpyrazol-1-yl)borate complexes appears to be crucial to the successful maintenance of mononuclearity at the Mo(V) level.

(40) Chen, G. J.-J.; McDonald, J. W.; Newton, W. E. *Inorg. Chim. Acta* **1979**, *35*, 93.

(41) In the cyanolysis reaction, sulfur atom transfer produces SCN^- and a Mo complex which undergoes aquation and CEPT reactions leading to the (hydroxo)oxo species. It appears that despite the favorable positioning of the dithiophosphinate ligand for chelation, a consequence of the weak intramolecular Mo=S···S=P interaction in the oxothio-complexes, the sterically undemanding SCN^- intermediate permits aquation to take place. In the phosphine reactions, the oxo−Mo(IV) complexes and $SPPh_3$ are produced in high yield. The egress of the $SPPh_3$ molecule from the coordination sphere provides sufficient steric protection from aquation, permitting the chelation of the dithiophosphinate ligand in this case. Laughlin, L. J.; Eagle, A. A.; Tiekink, E. R. T.; Young, C. G. Unpublished results.

Summary

This paper documents the synthesis, characterization and reactivity of a variety of oxo−Mo(IV) and dioxo−Mo(VI) complexes containing ambidentate dithiophosphinate and trispyrazolylborate ligands. These complexes catalyze biologically relevant OAT processes and are susceptible to redox, CEPT, and CENT reactions leading to mononuclear, EPR-active $[Mo^VO]^{3+}$, $[Mo^VO_2]^+$, $[Mo^VO(OH)]^{2+}$, and $[Mo^VOS]^+$ species having varying relevance to enzyme systems. The OAT reactions provide further indirect support for the oxo-transfer hypothesis[7,8] while the CEPT and CENT reactions model the generation of Mo(V) intermediates during enzyme turnover.[4] The oxidation of oxothio−Mo(V) complexes to oxothio−Mo(VI) species provides evidence for a key step in the mechanism proposed by Wahl and Rajagopalan[38] for the reactivation of desulfo xanthine oxidase by sulfide.

Acknowledgments. We thank Aston A. Eagle for helpful discussions and gratefully acknowledge the financial support of the Australian Research Council.

IC950815M

(42) Laughlin, L. J.; Gulbis, J. M.; Tiekink, E. R. T.; Young, C. G. *Aust. J. Chem.* **1994**, *47*, 471.